nature portfolio

https://doi.org/10.1038/s41589-021-00829-z

Supplementary information

Mechanical strength of RNA knot in Zika virus protects against cellular defenses

In the format provided by the authors and unedited

Supplementary Material for:

Mechanical strength of RNA knot in Zika virus protects against cellular defenses

Meng Zhao, Michael T. Woodside

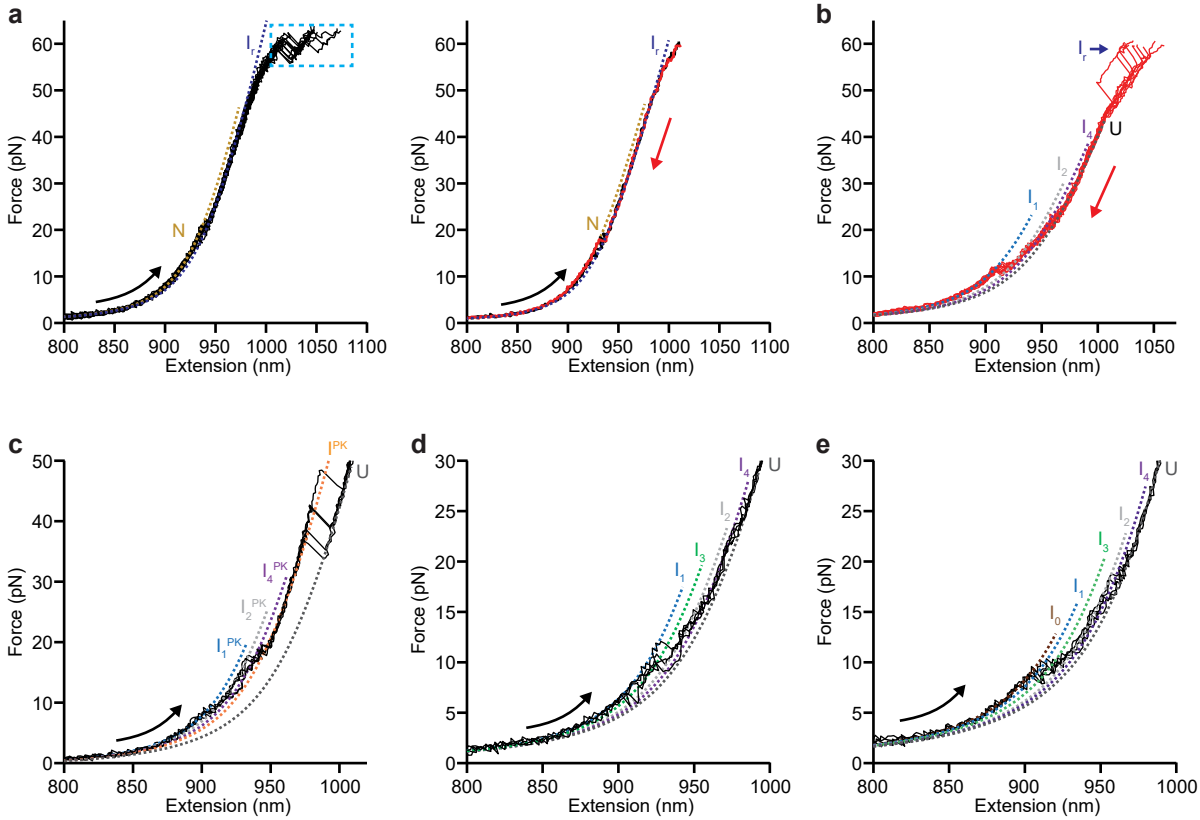

Supplementary Fig. 1: Representative FECs of wild-type Zika-xrRNA. (**a**) Multiple unfolding FECs (left panel) showing a mechanically resistant intermediate (I_r) that remains after partial unfolding of the native state (N). I_r unfolding usually required pulling the construct into the overstretching transition at ~60 pN (cyan dashed box), such that the unfolding transition could not be distinguished from overstretching. If the unfolding force was not maintained at ~60 pN for long enough during unfolding (right panel, black), then I_r typically stayed intact (was not unfolded) and the RNA returned directly to N in the subsequent refolding FEC (red). (**b**) In some FECs, I_r remained folded at the beginning of the refolding curve but subsequently unfolded to U while the force remained elevated. Such cases indicated that the 2-s waiting time at the overstretching transition was not always sufficient to ensure that I_r always unfolded. After the unfolding event on the refolding curve, refolding from U into I_1 was seen to occur through the usual series of intermediates (in this case, I_4 and I_2). (**c**) Representative unfolding FECs indicating a structure containing the pseudoknot without 5′-end threading, I_1^{PK}, which unfolds through distinct intermediates I_2^{PK}, I_4^{PK} and I^{PK}. The first 3 unfolding events occurring at low force involve unfolding of secondary structure only, respectively P1, P2, and P4. Because of the lack of 5′-TC, P1 does not participate in any tertiary structure and unfolds at low force, unlike in N. (**d**) Representative FECs showing unfolding of native secondary structure only. (**e**) Representative FECs showing unfolding of secondary structure only but including an additional non-native helix in intermediate I_0. Dotted curves show WLC fits to each state.

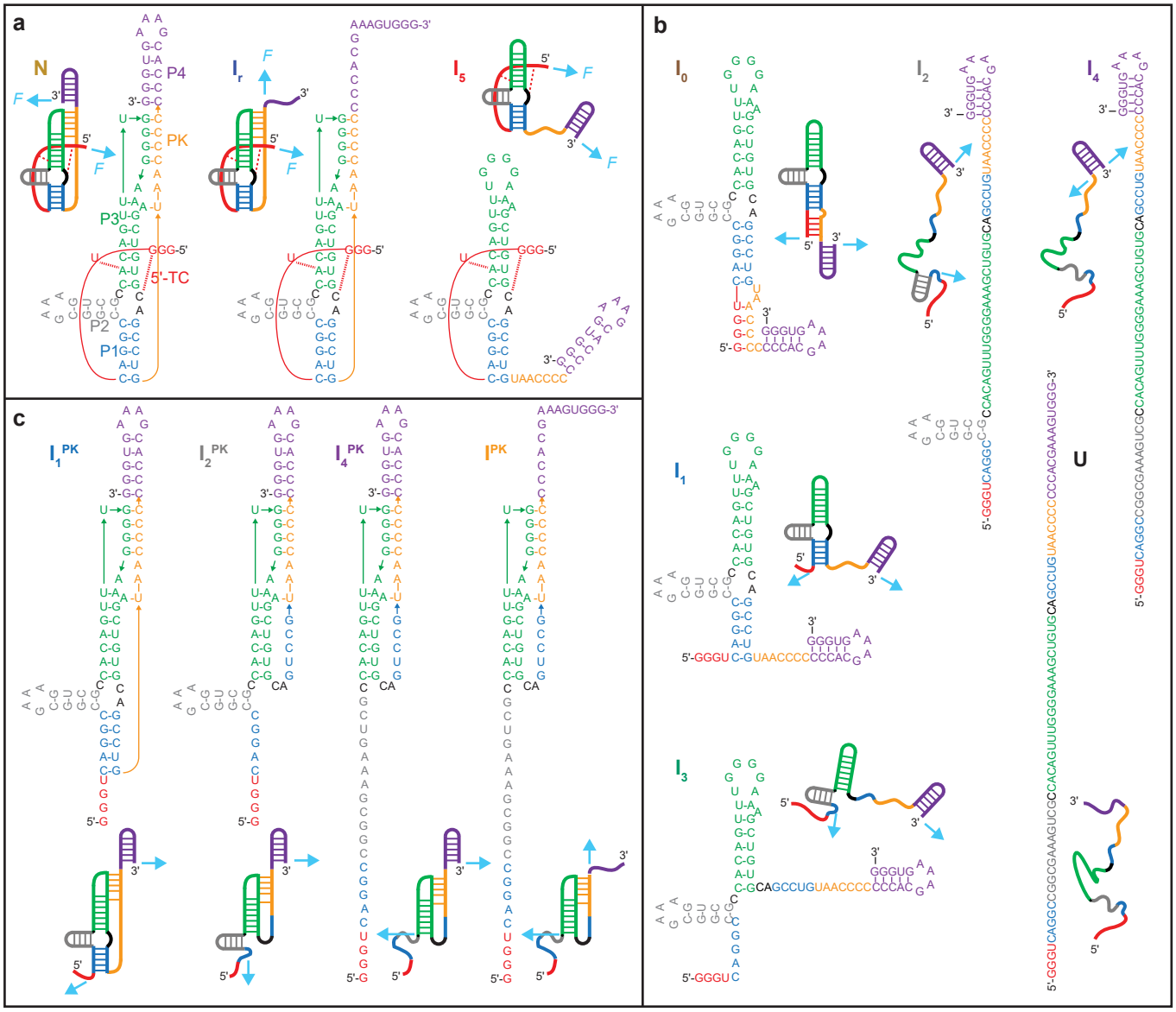

Supplementary Fig. 2: Structural models of states on unfolding and refolding pathways for wild-type Zika xrRNA under native conditions. (**a**) States with tertiary contacts stabilizing threading of the 5′ end. (**b**) States containing only secondary structure. (**c**) States containing pseudoknots but no threading of the 5′ end. The color coding is the same as in Fig. 1. Contour length changes expected from unfolding each structure are listed in Supplementary Table 2. Cyan arrows indicate the locations within each structure where the tension from the optical tweezers is applied.

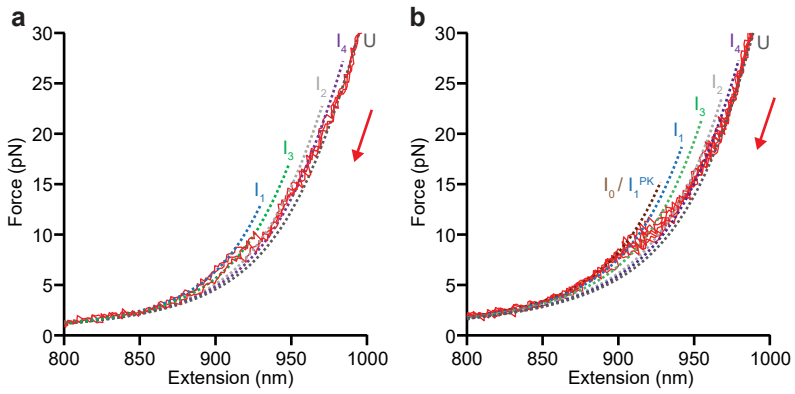

Supplementary Fig. 3: Refolding FECs. (**a**) Refolding FECs leading into state I_1 show sequential formation of each helix. (**b**) Refolding FECs leading into I_0 or I_1^{PK} show a similar pattern, with an additional transition at low force. States I_0 or I_1^{PK} cannot be distinguished in refolding FECs, because their ΔL_c values are too similar (Supplementary Table 2); they can only be distinguished in unfolding FECs by their unfolding forces. Dotted curves show WLC fits to each state.

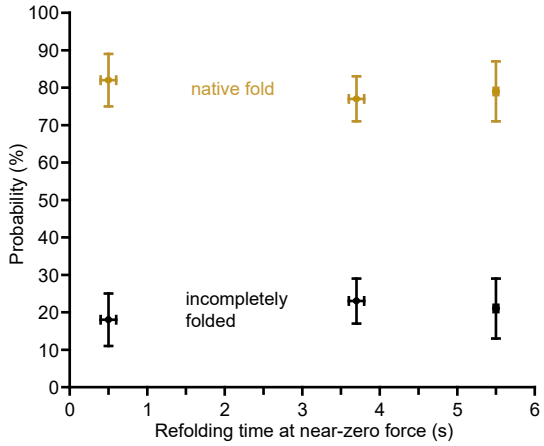

Supplementary Fig. 4: Effect of waiting time near zero force on xrRNA unfolding. The probability of finding the xrRNA in the native state (gold) as opposed to one of the incompletely folded states (black) is the same within error whether waiting 0.5 s near zero force between subsequent unfolding/refolding cycles (601 FECs from 17 molecules), 3.7 s (975 FECs from 35 molecules), or 5.5 s (1030 FECs from 19 molecules). Error bars represent s.e.m.

Supplementary Table 1: RNA and DNA sequences. Sequences of wild-type and mutant Zika xrRNA constructs (mutations shown in blue) and anti-sense DNA oligonucleotides used for SMFS and Xrn1 digestion assay. The leader and downstream sequences of the xrRNA constructs used for the Xrn1 digestion assays are shown in italics. The spacer oligo and complementary sequences in the RNA constructs for digestion assays are underlined.

Assay	Name	Sequence (5′→3′)
SMFS	wild-type xrRNA	GGG UCA GGC CGG CGA AAG UCG CCA CAG UUU GGG GAA AGC UGU GCA GCC UGU AAC CCC CCC ACG AAA GUG GG
	C22G mutant	GGG UCA GGC CGG CGA AAG UCG GCA CAG UUU GGG GAA AGC UGU GCA GCC UGU AAC CCC CCC ACG AAA GUG GG
	U4C mutant	GGG CCA GGC CGG CGA AAG UCG CCA CAG UUU GGG GAA AGC UGU GCA GCC UGU AAC CCC CCC ACG AAA GUG GG
	oligo 1	CTT TCG TGG G
	oligo 2	CTT TCG TGG GGG GGT TA
	oligo 3	GCC TGA CCC
Xrn1 digestion	wild-type xrRNA	*GGG CCU CCG GAC UCU AGC GUU UAA ACU UAA GCU U* GG GUC AGG CCG GCG AAA GUC GCC ACA GUU UGG GGA AAG CUG UGC AGC CUG UAA CCC CCC CAC GAA AGU GGG *GGA UCC ACU AGU CCA GUG UGG UGG AAU UC*
	U4C mutant	*GGG CCU CCG GAC UCU AGC GUU UAA ACU UAA GCU U* GG GCC AGG CCG GCG AAA GUC GCC ACA GUU UGG GGA AAG CUG UGC AGC CUG UAA CCC CCC CAC GAA AGU GGG *GGA UCC ACU AGU CCA GUG UGG UGG AAU UC*
	spacer	*GCT TAA GTT TAA ACG C*

Supplementary Table 2: Contour lengths for wild-type Zika xrRNA unfolding and refolding. For each of the states identified in the unfolding and refolding FECs, from each of the three types of pathways observed (ring-knot, unthreaded pseudoknot, helices-only), the contour lengths relative to the native ring-knot, L_c, are listed. The values observed (using a weighted average of the results from unfolding and refolding FECs) are compared to the values expected for the proposed structures based on the crystal structure. Errors in the observed contour length represent the standard error on the mean (total of 5212 FECs from 69 molecules).

Pathway	Pathway occupancy	State	Observed L_c (nm)	Expected L_c (nm)
Ring-knot • 5′ end threaded • ring closed	80%	N	0[a]	0
		I_r	6.1 ± 0.4	6.1
		I_1	6.9 ± 0.8	7.3
		I_2	26 ± 1	27.3
		I_4	31.0 ± 0.9	32.2
		U	38.2 ± 0.6	38.3
Pseudoknot ○ 5′ end unthreaded • ring closed	4%	I_1^{PK}	2 ± 1	2.0
		I_2^{PK}	9.3 ± 0.9	9.3
		I_4^{PK}	15.4 ± 0.8	15.9
		I^{PK}	21.7 ± 0.7	22.0
		I_4	33 ± 1	32.2
		I_2	28 ± 1	27.3
		I_3	17 ± 1	17.0
		U	38.3[a]	38.3
Helices only ○ 5′ end unthreaded ○ ring open	16%	I_0	1.4 ± 0.5	1.4
		I_1	7.0 ± 0.8	7.3
		I_3	16 ± 1	17.0
		I_2	25.9 ± 0.6	27.3
		I_4	31.7 ± 0.8	32.2
		U	38.3[a]	38.3

[a] Value fixed during WLC fitting to generate L_c for the other states in the same FECs.

Supplementary Table 3: Contour lengths in presence of anti-sense oligos or absence of Mg^{2+}. Observed and expected contour lengths relative to the native ring-knot are listed for each state on each pathway observed in each of four conditions: the presence of anti-sense oligos 1–3 or absence of Mg^{2+}. Weighted averages from unfolding and refolding FECs are compared to the values expected for the proposed structures. Errors represent s.e.m.

Condition	Number of molecules	Number of FECs	Pathway occupancy	State	Observed L_c (nm)	Expected L_c (nm)
oligo 1	16	4552	90%	I_r	6.2 ± 0.6	6.1
			0.3%	I_{5b}	11.8 ± 0.7	11.3
			10%	I_{1b}	13.1 ± 0.4	13.4
				I_{3b}	23.4 ± 0.4	23.1
				I_{2b}	33.4 ± 0.8	33.4
oligo 2	5	1462	41%	I_{5b}	12 ± 1	11.3
			59%	I_{1b}	13.8 ± 0.8	13.4
				I_{3b}	24 ± 1	23.1
				I_{2b}	32 ± 1	33.4
oligo 3	8	1930	100%	I_3	16 ± 1	17.0
				I_2	26 ± 1	27.3
				I_4	32 ± 1	32.2
No Mg^{2+}	11	796	33%	$I_0^{PK'}$	5 ± 1	4.9[a]
				$I_1^{PK'}$	11 ± 1	9.6[a]
			67%	I_1	6 ± 1	7.3
				I_2	26 ± 1	27.3
				I_4	31 ± 1	32.2

[a] PK′ is non-native and hence d_T could not be measured directly from the crystal structure. It was estimated as 2.0 nm for $I_0^{PK'}$ (distance between G32 and C60) and 4.4 nm for $I_1^{PK'}$ (distance between C5 and C60).

Supplementary Table 4: Contour lengths for C22G mutant. Contour length L_c (relative to N^{m1}) of states identified in unfolding and refolding FECs of the C22G mutant, compared with expected values. Observed/expected contour lengths are listed for each state identified on each pathway for the two isomers with different G22 base-pairing. Weighted averages from unfolding/refolding FECs are compared to the values expected for the proposed structures. Errors represent s.e.m (1414 FECs from 11 molecules without oligo, 469 FECs from 2 molecules with oligo 3).

Isomer	Pathway occupancy	State	Observed L_c (nm)	Expected L_c (nm)
Without anti-sense oligo				
C9:G22	15%	N^{m1}	0	0
		I_r^{m1}	6.0 ± 0.6	6.1
	53%	I_1''	7.3 ± 0.7	7.3
		I_4''	25.3 ± 0.6	26.1
		I_2''	31.0 ± 0.6	32.2
G22:C44	17%	I^{m1}	9.8 ± 0.6	9.0[a]
	15%	I_1'	8.0 ± 0.5	7.3
		I_3'	18.1 ± 0.5	17.2
		I_2'	27.7 ± 0.7	28.5
		I_4'	30.5 ± 0.6	32.2
With oligo 3				
C9:G22	100%	I_3''	15.4 ± 0.8	15.9
		I_4''	26.4 ± 0.7	26.1
		I_2''	32.1 ± 0.6	32.2

[a] Because the pseudoknot in I^{m1} is non-native, d_T cannot be measured directly from the crystal structure. It was estimated as 4.3 nm (distance between U4 and C60).

Supplementary Table 5: Contour lengths for U4C mutant. Contour length L_c (relative to N^{m2}) of states identified in unfolding and refolding FECs of the U4C mutant, compared with expected values. The observed and expected contour lengths relative to the state N^{m2} are listed for each state identified on each pathway observed for the four conformers. Weighted averages from unfolding FECs are compared to the values expected for the proposed structures. Errors represent s.e.m (total of 450 FECs from 5 molecules without oligo, 162 FECs from 2 molecules with oligo 2).

Pathway	**Pathway occupancy**	**State**	**Observed L_c (nm)**	**Expected L_c (nm)**
Without anti-sense oligo				
Ring-knot	52%	N^{m2}	0[a]	0
• 5′end threaded		I^{m2}	7.6 ± 0.7	6.1
• ring closed		U	37.6 ± 0.4	38.3
Helices only	44%	I_1	8.5 ± 0.9	7.3
		I_3	18 ± 1	17.0
○ 5′end unthreaded		I_2	26.2 ± 0.6	27.3
○ ring open		I_4	31.1 ± 0.8	32.2
		U	38.3[a]	38.3
Open ring-knot	1%	$I_5{}^{m2}$	6 ± 1	5.2
• 5′end threaded		$I_{5b}{}^{m2}$	12.9 ± 0.8	11.3
○ ring open		U	38.3[a]	38.3
Open ring-knot	3%	I_6	7 ± 1	5.8[b]
○ Non-native 5′TC (G3:C22) folded?		I_7	19.1 ± 0.8	N/A
		I_8	28.0 ± 0.7	N/A
○ ring open		U	38.3[a]	38.3
With oligo 2				
Helices only	27%	I_{1b}	13.0 ± 0.6	13.4
		I_{3b}	24.1 ± 0.7	23.1
○ 5′end unthreaded		I_{2b}	33.2 ± 0.6	33.4
○ ring open		U	38.3[a]	38.3
Open ring-knot	73%	$I_{5b}{}^{m2}$	12.2 ± 0.7	11.3
• 5′end threaded		U	38.3[a]	38.3

[a] Value fixed during WLC fitting to generate L_c for the other states in the same FECs. [b] The structure for I_6 is speculative; d_T was estimated as 1.8 nm using the distance between G3 to C44 from the crystal structure.